Physicochemical and Biopharmaceutical Characterization of N-Iodomethyl-N,N-Dimethyl-N-(6,6-1 Diphenylhex-5-En-1-Yl) Ammonium Iodide and A Promising Antileishmania Delivery System

Maritza Fernández[1], Luz Amalia Ríos-Vásquez[2], Rogelio Ocampo-Cardona[2], Oscar Flórez[3], David L Cedeño[4], Teresa M Garrigues[5], Antonio J Almeida[6], Iván D Velez[1] and Sara M Robledo[1*]

[1]*Facultad de Medicina, Universidad de Antioquia, Medellín, Colombia*

[2]*Departamento de Química, Universidad de Caldas, Manizales, Colombia*

[3]*Facultad de Ciencias Farmacéuticas y Alimentarias, Universidad de Antioquia, Medellín, Colombia*

[4]*Department of Basic Science Research, Millennium Pain Center, Bloomington, USA*

[5]*Departamento de Farmacia y Tecnología Farmacéutica y Parasitología, Universidad de Valencia, Valencia, Spain*

[6]*Facultad de Farmacia, Universidad de Lisboa, Lisboa, Portugal*

*Corresponding author: *Sara M Robledo, PECET, Facultad de Medicina, Universidad de Antioquia UdeA, Calle 70 # 52-21, Medellín, Colombia*

Abstract

Cutaneous leishmaniasis (CL) is an infectious disease endemic in tropical and subtropical countries. The current drugs have severe drawbacks that restrict their use and enhance the need for better drugs. Recently, the N-iodomethyl-N,N-dimethyl-N-(6,6-diphenylhex-5-en-1-yl) ammonium iodide (C_6I) was identified as a promising compound for the topical treatment of CL. The need for oral drugs with potential use to treat cutaneous, mucosal and visceral leishmaniasis, in the present work were determined the pharmaceutical and some biopharmaceutical properties of C_6I as possible oral treatment and based on this results a nanoformulation was elaborated, characterized and tested in *in vitro* and *in vivo* model of the antileishmanial activity and toxicological assays. The C_6I showed crystalline form and good intestinal permeability, its dissolution profile did not change with pH changes. The C_6I was not mutagenic and genotoxic *in vitro*, it presented some minors acute toxicological effects.

The solid lipid nanoparticles (SLN) used Precirol® as lipid, it had a size in the nano range scale with a low polydispersity index, and encapsulation efficiency > 60%. The nanoparticles of C_6I (PC_6I) increased the *in vitro* antileishmanial activity 40-fold than free C_6I. In turn, the oral administration of C_6I and PC_6I (30 mg/kg/d, 28 days) produced complete cure in 42.9% and 71.4%, respectively, with no relapses and no toxicity. The effectiveness of meglumine antimoniate was 100% but the relapse rate was 28.6%. C_6I and PC_6I are safe compounds, as demonstrated in *in vitro* and *in vivo* assays for toxicological profile. In conclusion, a novel oral quaternary ammonium iodide salt-based formulation with antileishmanial properties was developed. The safety and effectiveness information of PC_6I formulation showed here supports the further evaluation of efficacy and safety in patients to validate the use of PC_6I as an alternative for the oral treatment of CL.

Keywords

Cutaneous leishmaniasis, Quaternary halomethylated ammonium iodide, Drug development, Solid lipid nanoparticles, Precirol®

Introduction

Current drug therapies for cutaneous leishmaniasis (CL) are unsatisfactory due to numerous drawbacks including severe side effects, reproductive toxicity, prolonged treatment with high doses and decreased effectiveness. Since CL is prevalent in economically dis-

Fernández et al. Int Arch Med Microbiol 2018, 1:007

• Page 1 of 14 •

advantaged communities, new drugs development lack for economic incentives to large pharmaceutical companies and in consequence, leishmaniasis is designated as neglected tropical disease [1,2].

In a previous work was reported that the quaternary halomethylated ammonium salt N-iodomethyl-N,N-dimethyl-N-(6,6-diphenylhex-5-en-1-yl) ammonium iodide (C_6I), a choline analog, could be considered as a lead compound in the development of a new treatment for CL. The C_6I has activity against intracellular amastigotes of *Leishmania (Viannia) panamensis* [3,4]. Moreover, the C_6I administered topically at a dose of 2 mg/kg/day during 15 days was able to cure hamsters with experimental CL caused by *L. (V) braziliensis* [5]. The ability of C_6I to inhibit the choline/ethanolamine kinase of *L. (Leishmania) infantum* and the production of phosphatidyl choline and to interfere with the *in vitro* uptake of choline by promastigotes of *L. tarentolae* was also demonstrated [6]. The organoleptic analyses showed that C_6I is an odorless, white-colored powder with fine appearance, soft to the touch, crystalline habits with regular plaque shapes and smooth texture, grouped in clusters and particle size varying between 20 and 100 microns. Other physiochemical studies showed that the solubility of C_6I is high in acetonitrile (1.5 mg/mL), low in methanol, isopropanol and chloroform (< 1.0 mg/mL) and water (0.61 mg/mL). This solubility is not affected by pH changes [5].

The importance of C_6I is higher when considering the urgency expressed by the World Health Organization of having drugs for oral administration since miltefosine, the only medicine available for oral treatment of leishmaniasis, is not widely available in the market.

In the present work were determined the pharmaceutical properties of C_6I as well as the usefulness of oral C_6I to cure experimental CL in hamsters. The *in vitro* cytotoxicity, mutagenicity and genotoxicity of C_6I were also determined. Because the low solubility observed previously for C_6I could difficult the dissolution process in the GI tract and, affect the bioavailability [7], the oral delivery can be improved using nanocarrier systems such as solid lipid nanoparticles (SLNs) that are at the forefront of the potential application mainly due to the low cost and easy industrial production [8]. Thus, in the present work were prepared and characterized SLNs of C_6I using Precirol® (PC_6I). The *in vitro* and *in vivo* antileishmanial toxicity and activity of PC_6I were assessed against *L. (V) braziliensis*, compared to the antileishmanial activity of free C_6I and with the standard treatment to this disease, meglumine antimoniate (MA). Finally, the *in vivo* oral toxicity profile was also determined.

Materials and Methods

Compound

The C_6I was supplied by L.A Rios and R. Ocampo. Its synthesis was previously described by Duque, et al. 2016 [3].

Ethical aspects

The study for intestinal absorption was approved by the Ethical Committee for Animal Welfare of the University of Valencia (Act No. CE 86/609) while the *in vivo* assays for, *in vivo* effectiveness and toxicity, maximum tolerable dose and oral toxicity at repeated dose were approved by the Ethical Committee for Animal Experimentation of the Universidad de Antioquia (Act No. 91-2014).

Biopharmaceutical and pharmacological parameters of C_6I

Intrinsic dissolution: One hundred mg of C_6I were compressed at 700 Pa and a 6.33 mm punch during 1 min. The surface area of the compacts was 3.14 cm^2 [9]. Compacts were placed in a molten beeswax-mold with one face in contact with dissolution medium. Dissolution was conducted in an USP type 2 dissolution apparatus using 900 mL of either 0.1 N HCl, 0.2 M acetate buffer, pH 1.5, purified water pH 7.0 and 0.2 M phosphate buffer, pH 8.0 at 37 ± 1 °C, as dissolution media, respectively, with a paddle rotating at 100 rpm. One mL samples were withdrawn at regular intervals and a plot of absorbance *vs.* time was constructed. Experiments were done in triplicate. Absorbance was determined using the UV-Vis spectrophotometer (VarioScan Thermo) at 233. The dissolved cumulative amount per surface unit of the compact was plotted against time for each vessel. A standard curve was built using standard solutions used in dissolution media. Intrinsic dissolution rate (IDR) was calculated using Eq. 1:

$$j = V \frac{dct}{dt(\frac{1}{A})} \qquad (1)$$

Where j is the IDR, V is the volume of the dissolution medium, c is the concentration, A is the area of the C_6I disk and t is the time

Thermic properties and powder X-ray diffraction: The melting points, purity and crystalline appearance of C_6I were determined by differential scanning calorimetry (DSC) profile using a DSC 204 F1 (Phoenix®-NETZSCH-Gerätebau GmbH). Measurements were in a range of 25 °C to 300 °C with increases in 10 °C per min. The temperature scale was calibrated using an internal reference within pots of aluminum. Tests were performed in a nitrogen atmosphere.

The crystallinity properties of C_6I were determined by Powder x-ray diffraction (PXRD) using an X-ray diffractometer Rigaku Miniflex® (Rigaku, Tokyo, Japan) with a source of Cu, Ka1 radiation (1.542 A°) and angles ranging between 3° and 50°.

***In situ* intestinal absorption by doluisio method:** Thirteen adult Wistar male rats were fasted for 18 h (except for drinking) and then anesthetized and immobilized. Afterwards, the abdominal cavity was cut along

the medioventral line, and the small intestine was separated. Then, the small intestine was washed with 0.9% saline solution and two different concentration of compound was used, 10 mL of supersaturated or 1/10 diluted C_6I solution were perfused. The concentration of C_6I in the intestinal lumen was measured every 5 min for 30 min by sampling 200 µL of the remaining liquid. Samples were immediately centrifuged (1,500 g, 10 min) and the supernatant frozen (-80 °C) until quantification by HPLC using the method described [5]. Samples of 1.0 mg/mL of C_6I were prepared and run in an Agilent Technologies 1200 chromatograph equipped with a C18 column (Restek C18, 5 µm, 250 × 4.6 mm), with UV-detector. The mobile phase consisted of acetonitrile and C_2H_3N-aO_2 0.1 M (60:40, v/v), adjusted to pH 5.0 with acetic acid. Elution was achieved in 12 min at a flow rate of 0.8 mL/min. The injection volume was 10 µL. Compound was monitored at 233 nm. At the end of the sampling, the remaining volume was recovered and the extent of water reabsorption was determined at every sampling time, considering that this process follows zero-order kinetics [10]. The apparent constant absorption rate for C_6I was obtained from the first-order equation Eq. 2:

$$c = c_o e^{-k_a t} \qquad (2)$$

Where C is the concentration of C_6I remaining in the intestinal lumen, k_a is the apparent rate constant for absorption, and C_0 is the initial concentration of C_6I.

The k_a was transformed in to permeability values by means of Eq. 3:

$$papp = \frac{ka * R}{2} \qquad (3)$$

Where R is the effective radius of the intestinal segment corresponding to 0.1784 cm, considering that intestinal segment as a cylinder of 10 mL volume and 100 cm length.

***In vitro* mutagenicity:** *Salmonella typhimurium* TA98 and TA100 adjusted at $2 × 10^9$ CFU/mL and 100-µL were added to assay tubes containing C_6I (46, 23 and 12 µg/mL) and 500 µL of phosphate buffer (Na_2HPO_4 and $NaH_2PO_4 \cdot H_2O$) - system without metabolic activation -, and pre-incubated at 37 °C for 30 min. Sodium azide (AzNa) or 4-Nitroquinoline (4NQO) (5 µg/mL) were used as positive control for *S. typhimurium* TA100 and TA98 strain, respectively. Phosphate buffer was used as negative control. Revertants (his+) were counted after incubation at 37 °C for 66 h [11].

***In vitro* genotoxicity:** Chromosome alterations induced by C_6I were evaluated in lymphocytes from three healthy donors [12]. Cells cultured in RPMI 1640 medium supplemented with 2 mM L-glutamine, 10% fetal bovine serum and 1% penicillin-streptomycin (10,000 U-10 mg/mL) (complete medium) were stimulated with 200 µL phytohemagglutinin and incubated at 37 °C, 5% CO_2. After 36 hours, the cells were treated with each of sublethal C_6I concen-

trations (46 - 23 and 12 µg/mL) and incubated during 24 h. Colcemid (0.1 pg/ml) was added and cells were incubated again during 1 h. The cells were centrifuged, resuspended in 0.075 M KCl and incubated at 37 °C for 7 min, fixed 10 min with Carnoy solution, washed and dripping. Slides were dried and stained with 5% Giemsa, pH 6.8. One hundred metaphase cells (46 chromosomes) were analyzed. Structural chromosome aberrations were classified as chromatid breaks (B), chromosome breaks (BB), dicentric chromosomes (DC), ring chromosomes (R) and multiradial chromosomes (MR). Each treatment was performed in two separate experiments using RPMI as negative control and mitomycin-C (10 M) as positive control.

Maximum tolerable dose of C_6I: Twenty-one female, nulliparous and non-pregnant Wistar rats, 188 ± 12 g weight, were divided into four groups. Three groups (n = 6 each) were treated with a single dose of 5, 50 or 300 mg/kg (1 mL) of C_6I by the oral route. The forth group (n = 3) received distilled water (control group). Rats were observed during the first 6 h for any potential signs of toxicity and then daily during 14 days. Signs were graded according their nature and severity. Rats were weighed before and every week after doses. At day 14 rats were sacrificed and necropsied. The heart, brain, liver, spleen, kidneys, testicles and epididymis (males) and ovaries (females) were weighed and biopsies were stored in 10% formaldehyde for histopathology analysis [13]. The severity of lesions was graded from 0 to 3, where 0 for no lesion, mild, moderate or severe, respectively. The surviving rats were monitored for mortality, behavior, fur, pain and any sign of illness during the study.

Development and characterization of solid lipid nanoparticles

The Precirol® lipid was selected because it is frequently used in oral formulation, the production method of SLN was selected, first to determine of solubility of C_6I in Precirol®, one milligram of compound was added to 25 mg of lipid that was heated above 10 °C its melting points. Solubility was verified after that the excess of C_6I persisted for more than 8 hours [14].

The Precirol® NPs loaded with C_6I (PC_6I) were elaborated by evaporation of the emulsion-solvent using 0.6% sodium deoxycholate, 0.5% Tween 20 and 1% soy lecithin as co-surfactants [15]. Fifty mg of Precirol® was dissolved with lecithin and C_6I (3 mg) in 1 ml of dichloromethane. This organic phase was then added to 5 mL of aqueous phase containing Tween 20 and sodium deoxycholate. Dispersion was performed by sonication for 3 min (Branson Sonifier 250, USA) followed by 5 min of stirring at 12,500 rpm for 4 h at room temperature using a High Speed Mixer (Model L4RT, Silverson Machines, Chesham, UK) until the dichloromethane had completely evaporated. Free C_6I was separated from the dispersed Precirol® NPs by size exclusion chromatography in a PD-10 column (Bio-Rad Laboratories) using as eluent phosphate buffer saline (PBS), pH 7.4.

The NPs were characterized based on particle size and surface charge (PZs) determined by photon correlation spectroscopy (PCS) using a Zetasizer Nano S (Malvern Instruments, UK). Measurements of particle size were performed at 25.0 ± 0.1 °C after dilution of the NPs in purified water (1:100). The results were expressed as the average of particle size and the polydispersion index (PI). In turn, the surface PZ value of the NPs was determined based on the mobility of the particles in an electric field using a Zetasizer Nano Z. For this, the diluted samples in purified water were exposed to 150 mV and the appearance.

The incorporation of C_6I into the NPs was quantified after dissolving the NPs loaded with C_6I in acetonitrile, which promoted precipitation of the lipid phase. After centrifuging, free C_6I was measured at 233 nm in a microplate spectrophotometer (FLUOstar Omega). The supernatant from unloaded NPs was used as a blank. The quantification method was validated according to the international guide for validation of analytical procedures [16]. The efficiencies of encapsulation (EE) of C_6I and drug loading (DL) in the NPs were calculated according to Eq. 4 and Eq. 5:

$$(EE\%) = \frac{mg\ of\ encapsulated\ C61}{mg\ of\ initial\ C61}\ X\ 100 \qquad (4)$$

$$(DL\%) = \frac{mg\ of\ encapsulated\ C61}{mg\ of\ lipid}\ X\ 100 \qquad (5)$$

The morphology of the NPs were determined by scanning electron microscopy (SEM, XL-30 Royal Philips Electronics, Amsterdam). All measurements were performed in triplicate.

Stability of solid lipid nanoparticles loaded with C_6I: Five mL aliquots of PC_6I in suspension were stored at 2-8 °C, and the mean particle diameter, PI, zeta potential and DL were determined after 30 and 60 days of storage. The average of particle size was analyzed as previously described. The stability evaluation in terms of EE and DL was determined after separation of unbound C_6I by size exclusion chromatography, as described above. The effect of autoclaving was also evaluated, for this assessment, the PC_6I formulation was divided into two aliquots of equal volume. One aliquot was autoclaved at 121 °C for 20 min, while the other aliquot was maintained at 2-8 °C as a reference sample and then, the physicochemical properties (particle diameter, PI, surface charge, DL and EE) were compared. Additionally, the influence of temperature on the physical stability of PC_6I was evaluated using DLS (Zetasizer Nano S). Samples were diluted with purified water (1:100) in a quartz cell, and particle size analysis was performed while heating the sample from 25 °C to 90 °C at a rate of 0.5 °C/min and then cooling it from 90 °C to 25 °C at the same rate. Particle size was measured every 0.5 °C. This assay was done in triplicated.

Release of C_6I in solid lipid nanoparticle: The NPs were incubated in 10 mM PBS release medium, pH 7.4, with horizontal shaking at 37 °C. At 0.5 - 1 - 2 - 4 - 8 and 24 h intervals samples were centrifuged at 30,000 × g for 30 min at 4 °C. The released C_6I was quantified in the supernatants by spectrophotometry in a UV-1700 microplate reader at 233 nm. Quantifications were done in triplicate [15].

Differential scanning calorimetry (DSC): The DSC measurements were performed on a DSC calorimeter Q200 (TA Instruments, DE, USA). Dispersions of C_6I, Precirol®, sodium deoxycholate, Tween 20, soy lecithin, empty NPs and PC_6I nanoparticles were weighed and measured against an empty reference vessel. The samples were heated, and the respective thermograms were recorded in the temperature range of -20 °C to 240 °C at a heating rate of 10 °C/min.

Evaluation of efficacy and safety of C_6I and PC_6I

***In vitro* evaluation of cytotoxicity:** The cytotoxicity of free C_6I, empty NPs and PC_6I was evaluated *in vitro* on primary cultures of human monocyte-derived macrophages (MDMhu) and golden hamster peritoneal macrophages (MPha) and human cell lines U937 (ATCC® CRL-1593.2™), Caco-2 (ATCC® HTB-37™) and Detroit 551 (ATCC® CCL-110™). Cytotoxicity was determined by cell viability using the 3-(4,5-dimethylthiazol-2-yl)-2,5-diphenyltetrazolium bromide (MTT) enzymatic micromethod following a methodology described by others [17]. Untreated cells were used as a viability control and doxorubicin was used as a positive control for cytotoxicity. At least two independent experiments were performed, each in triplicate. The % of mortality was used to calculate the half maximal lethal concentration (LC_{50}) using the Probit analysis [18].

***In vitro* evaluation of anti-Leishmanial activity:** Intracellular amastigotes of *L. (V) braziliensis* (MHOM/CO/88/UA301-EGFP) were obtained after infection of U937 cells as described elsewhere [19]. After 24 h of infection the medium was replaced by fresh medium containing each C_6I, empty NPs or PC_6I, at concentrations of 100 - 12.5 - 3.125 - 0.78 µg/µL. After 72 h, cells infected and treated were analyzed by flow cytometry (FC 500MPL, Cytomics, Brea, CA, USA). The antileishmanial activity was determined according to the reduction in the number of viable parasites inside the infected cells obtained with each treatment and each concentration, according to the mean fluorescence intensity (MFI). Data obtained in untreated infected cells corresponds to 100% of parasites. All measurements were performed in triplicate, in two independent experiments. The half maximal effective concentration (EC_{50}) was calculated according to the Probit analysis [18].

Evaluation of *in vivo* effectiveness: Male and female hamsters, 6-weeks old, were inoculated in the dorsum with 5×10^8 promastigotes of *L. (V) braziliensis* (MHOM/

CO/88/UA301-EGFP)/100 mL. When the ulcer was developed in the skin, hamsters were distributed in five experimental groups. Two group of hamsters (n = 7 each) received by oral route 1 mL of C_6I or PC_6I at a dose of 30 mg/kg/day for 28 days. A third group (n = 7) was treated with MA at a dose of 120 mg/kg/day for 10 days, by intramuscular route, that corresponds to the curative dose identified in previous work (cure control) [20]. A fourth group (n = 3) was treated with the empty NPs (vehicle) and the fifth group (n = 3) remained untreated after infected (non healing control).

The clinical effectiveness of each treatment was determined by comparing the lesion sizes before treatment (TD0) with those observed the last day of treatment (TD28 for C_6I, PC_6I and NPs), or TD10 for MA) and days 30, 60 and 90 of follow-up after treatment (PTD30, PTD60 and PTD90, respectively). At the end of the study that is PDT90, the outcome was recorded as "cure" (complete disappearance of the lesion), "improvement" (more than 20% of decrease of the area), "failure" (increasing of the area), or "relapse" (reactivation of lesion after an initial cure). The parasitological effectiveness was also determined by quantification of parasite load in the skin samples from the ulcer at the end of the study (PTD90) by RT-PCR, following the protocol described by others [21].

Toxicity in hamsters after treatment: The toxicity of C_6I, PC_6I, NPs and MA was studied based on changes in the weight of hamsters measured every two weeks previous sedation. Additionally, at TD0 and day 8 after the end of treatment (PTD8) hamsters were bled by cardiac punction and serum was separated by centrifuging (5 min at 5,000 × g). Levels of alanine amino transferase (ALT), blood urea nitrogen (BUN) and creatinine (CRT) metabolites were quantified using commercial kits (Biosystems S.A, Barcelona, Spain). Hamsters were monitored daily for food and water consumption, activity and behavior. The appearance of fur, eyes and mucous membranes was also supervised.

Oral toxicity at repeated doses (28 days): Fifty healthy white Swiss Webster mice (CFW) of 18-22 g weight were divided into five groups (five males and five females, each). Two groups received 0.2 mL of C_6I or PC_6I at 30 mg/kg/day, respectively by oral route during 28 days. A third group remained untreated (negative control). Mice were monitored daily and weighted before treatment and weekly during treatment. Blood samples were obtained prior to the first dose (TD0) and at the end of the study (TD28) [22]. At the end of the study animals were sacrificed and necropsy and biopsies were performed. Serum level of aspartic transaminase (AST), ALT, BUN, CRT, albumin (ALB) and alkaline phosphatase (AP) were quantified. The blood cell parameters were also evaluated.

Statistical analysis

Data are expressed as mean ± SD, except for effectiveness of treatments that are expressed as percentage. The Kolmogorov-Smirnov test was used for normality distribution of data and differences between variables were analyzed by Student's t-test using GraphPad Prism version 6.0 (GraphPad Software, San Diego, CA, USA). Differences were considered significant when $p < 0.05$.

Results

Biopharmaceutical and pharmacological parameters of C_6I

Intrinsic dissolution: Intrinsic dissolution of pure compounds did not change with different pHs, the value of intrinsic rates (IDR) were similar in tree conditions, 0.24 ± 0.03 at pH 1.5; 0.26 ± 0.04 at pH 7.0 and 0.20 ± 0.05 at pH 8.0 (mg/min/cm²).

Thermic properties and powder X-ray diffraction: The DSC and powder X-ray diffractometric data are summarized in Figure 1. The C_6I had a melting point of 160.1 °C, an exothermic peak close to 150 °C, possibly due to the sublimation of iodine (Figure 1A) and an internal structure predominantly was crystalline confirmed by the XRPD analysis (Figure 1B).

***In situ* Intestinal absorption by Doluisio method:** The individual absorption rate constant (k_a) and *Papp* permeability values of C_6I obtained using a saturated solution and a 1/10 dilution solution were similar value
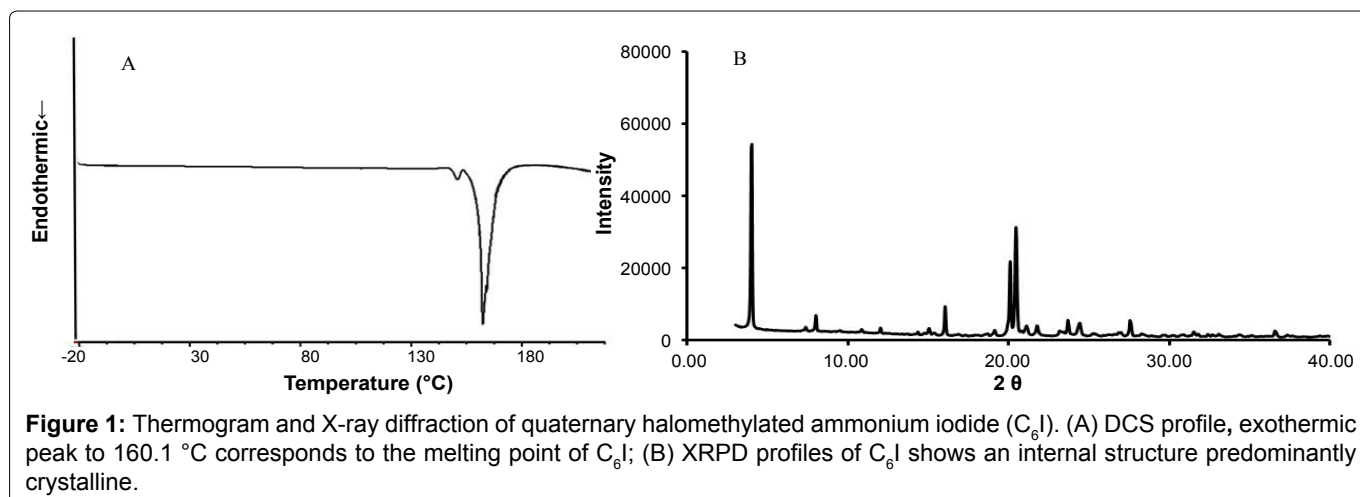

Figure 1: Thermogram and X-ray diffraction of quaternary halomethylated ammonium iodide (C_6I). (A) DCS profile, exothermic peak to 160.1 °C corresponds to the melting point of C_6I; (B) XRPD profiles of C_6I shows an internal structure predominantly crystalline.

without statistically significant differences, the permeability process in intestinal wall was independent of concentration (p > 0.05) (Table 1).

***In vitro* mutagenicity:** There was no significant increase in the number of revertant colonies of the TA98 and TA100 *S. typhimirium* strains in the three concentrations of C_6I compared to the negative controls. The test was done without exogenous metabolic activation system (p > 0.05). The positive controls AzNa and 4-NQO increased two times in the mutagenicity index compared to C_6I and negative control.

***In vitro* genotoxicity:** None structural chromosome aberrations were identified in the different concentrations of C_6I evaluated. No statistically significant differences were found between the subtoxic concentrations of C_6I and the negative control.

Maximum tolerable dose of C_6I: During the 14 days of observation after oral administration of three different concentrations of C_6I (5, 50 or 300 mg/kg), there were no deaths or evidence of clinical signs associated with severe toxicity or changes in the normal behavior of rats. A soft but not diarrheic stool was observed

a day after the compound C_6I was administered but it was normalized during the same day. A weight gain was observed in rats of all groups. There was no evidence of pathological signs during necropsy and no histological changes were confirmed. Therefore, it is possible to administer at one time a maximum concentration of pure compound of 300 mg/kg without significant effects.

Development and characterization of solid lipid nanoparticles

The C_6I was not soluble in Precirol® after fusion. Therefore, the formulation of PC_6I was prepared by emulsion and solvent evaporation processes. The particle size was homogeneous and this was range of nanometer, the encapsulation performance was 68% (2.04 mg of C_6I), and the PI values was lower than 0.3 (Table 2).

The SEM analyses showed that the NPs had spherical and homogeneous shape and some aggregates were present (Figure 2).

Stability of solid lipid nanoparticles loaded with C_6I: Storage of the NPs under refrigeration condition generated a slight decrease of the particle size of the NPs during the first month. On the other hand, the zeta potential increased in the first month but decreased in the second month. Unloaded NPs were not affected at the same extent by extensive refrigeration.

The heating processes by autoclaving did affect the particle sizes and the zeta potential decreased (Table 2). Additionally, DLS analysis showed that by increasing the temperature at 90 °C there was a gradual reduction in the particle size. Although the original size was not recovered after the cooling phase (Figure 3A), the heating and cooling process did not affect significantly of size of particles the values were always within the nano range.
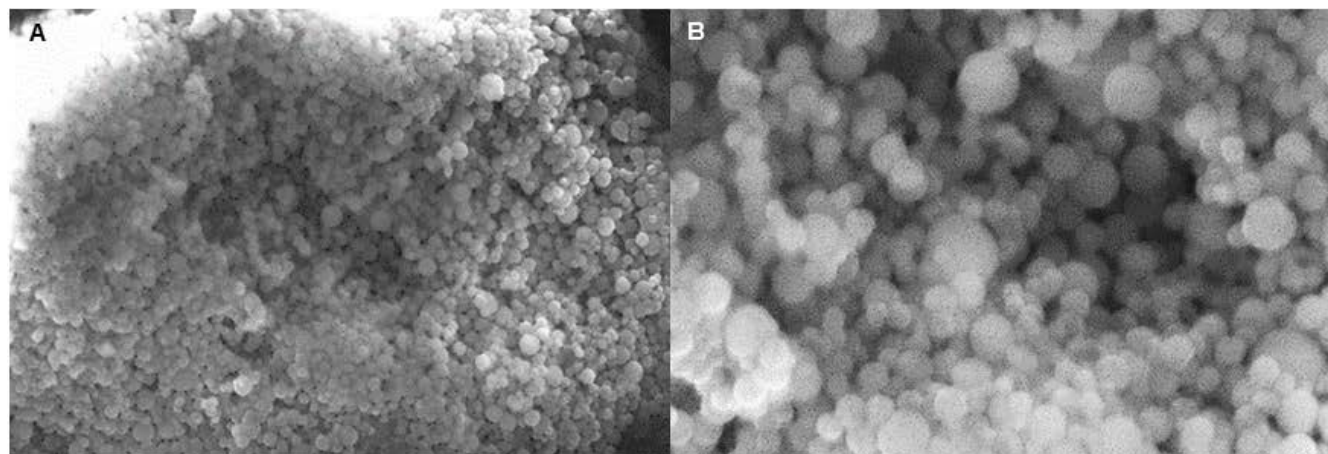
Table 1: Intestinal permeability of quaternary halomethylated ammonium iodide (C_6I).

Solution	Parameter	Mean ± SD
Saturated	k_a (h^{-1})	2.10 ± 0.4
	Papp (cm/s)	5.10×10^{-5} ± 1.0
	r^2	0.98 ± 0.01
1/10 diluted	k_a (h^{-1})	1.90 ± 0.37
	Papp (cm/s)	4.80×10^{-5} ± 0.9
	r^2	0.98 ± 0.005

Notes: With diluted solution only 6 animals were tested.

Abbreviations: k_a: Rate constant for absorption of the compound; Papp: Permeability value; r^2: Correlation coefficient.

Table 2: Physicochemical properties and stability of quaternary halomethylated ammonium iodide incorporated in Precirol® nanoparticles.

Conditions		Formulations	
	Parameters	Empty NPs	PC_6I
2-8 °C° T0	Size (nm)	112.5 ± 6.5	108.3 ± 2.2
	PI	0.2 ± 0.01	0.31 ± 0.03
	ZP mV	-25.7 ± 4.4	-16.4 ± 1.9
	%EE	NA	68.2 ± 0.03
	%DL	NA	13.7 ± 0.02
2-8 °C° T1	size (nm)	125.5 ± 1.5	103.1 ± 1.2
	PI	0.3 ± 0.2	0.3 ± 0.03
	ZP mV	-28.4 ± 0.5	-18.7 ± 2.8
2-8 °C° T2	size (nm)	133.3 ± 18.2	101.3 ± 5.1
	PI	0.3 ± 0.06	0.3 ± 0.04
	ZP mV	-18.4 ± 2.0	-8.6 ± 1.5
121°C*	Size (nm)	94.7 ± 7.4	86.7 ± 6.1
	PI	0.3 ± 0.01	0.2 ± 0.03
	ZP mV	-24.6 ± 2.9	-10.8 ± 1.4
	%EE	NA	62.8 ± 0.01
	%DL	NA	12.6 ± 0.04

Data represent mean value ± SD (n = 3). PC_6I: nanoparticles of Precirol® incorporating the quaternary halomethylated ammonium iodide C_6I; PI: polydispersion index; ZP: Zeta potential; EE: Encapsulation efficiency; DL: Drug loading. 2-8 °C° T0: Fresh NPs; 2-8 °C°; T1: One month stored; 2-8 °C° T2: Two month stored; NA: No apply. *during 20 min.

Figure 2: SEM images of quaternary halomethylated ammonium iodide incorporated in Precirol® nanoparticles (PC$_6$I). A) 2,350X. B) 7,000X. Notice of Spherical shape of nanoparticles.
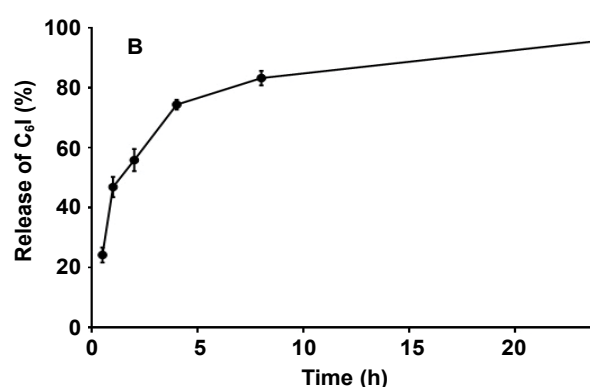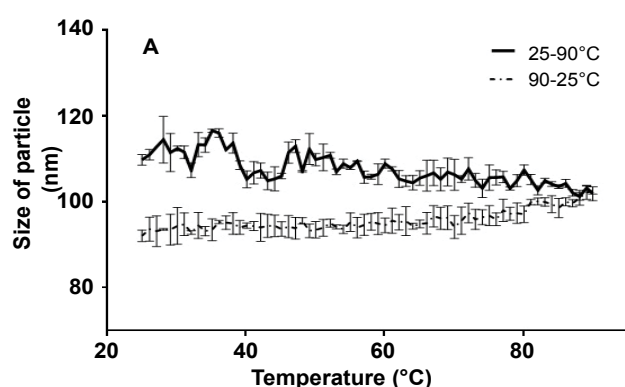

Figure 3: Release of quaternary halomethylated ammonium iodide from Precirol® nanoparticles *in vitro* and thermal analysis. (A) DLS thermogram of quaternary halomethylated ammonium iodide incorporated in precirol nanoparticles (PC$_6$I); (B) Release profile in 10 mM PBS pH 7.4 at 37 °C. data represent the mean value ± SD, n = 3.
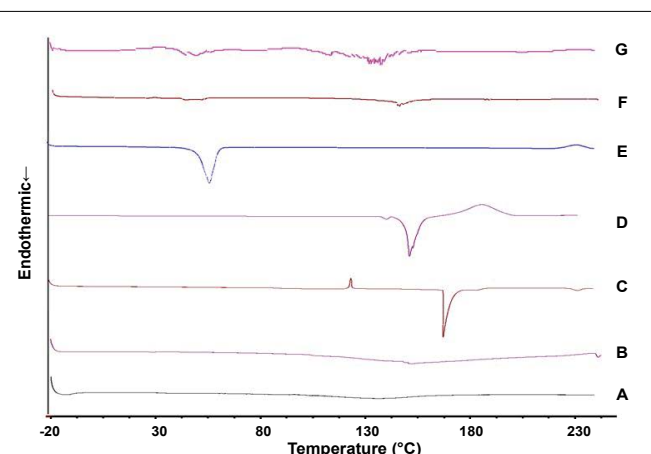

Figure 4: Thermograms of the components of Precirol® nanoparticles. (A) Tween 20, (B) lecithin, (C) sodium deoxycholate, (D) free C$_6$I, (E) Precirol®, (F) empty Precirol® nanoparticles, (G) Precirol® NP with C$_6$I.

Release of C$_6$I in solid lipid nanoparticle: There was a rapid release phase in the first 30 min followed by an exponential phase of release in the following 22 hours (Figure 3B). The efficiency of release of C$_6$I was ≥ 94% after 20 hours of observation. The quantification method for C$_6$I showed a sensitivity and accuracy according to the concentration range. The linearity varied from 0.03875 to 0.6 mg/mL, with a SD of 0.08 and a coefficient of variation of 3.1%. The limit of quantification (LOQ) and the limit of detection (LOD) were 0.03 and 0.009 mg/mL, respectively, with a confidence interval of 99.25%.

Differential scanning calorimetry (DSC): The melting point (mp) of Precirol® and C$_6$I were 70-80 °C and 163 °C, respectively. However, in the PC$_6$I, the melting point peak corresponding to C$_6$I was absent, possibly due to a structural change of the compound within the NPs from its crystalline form to an amorphous or molecularly dispersed state or the concentration of the compound is lower than of the lipid, which did not allow looking its peak. The Figure 4 shows the thermograms of each of the components of formulation, unloaded NPs and PC$_6$I.

Evaluation of toxicity and effectiveness of C$_6$I and PC$_6$I

***In vitro* cytotoxicity and antileishmanial activity:** To compare the results of free C$_6$I and encapsulated, first, the cytotoxic effects on fibroblast (Detroit 551) and MDMhu the doses was LC$_{50}$ < 100 µg/mL for C$_6$I while PC$_6$I was not cytotoxic for all the cell types evaluated, with a LC$_{50}$ > 200 µg/mL (Table 3). In relation with the effectivity, C$_6$I had an EC$_{50}$ 17.6 ± 1.0 µg/mL while PC$_6$I showed

Table 3: *In vitro* cytotoxicity and antileishmanial activity of free quaternary halomethylated ammonium iodide and incorporated in nanoparticles.

LC$_{50}$						EC$_{50}$	IS
Samples	haMP	huMDM	Detroit 551	Caco-2	U-937		
C$_6$I	9.5 ± 0.3	> 200	39.3	> 200	9.5 ± 0.2	17.6 ± 1.0	0.53
PC$_6$I	> 200	> 200	> 200	> 200	> 200	0.4 ± 0.2	500
NPs	> 200	> 200	> 200	> 200	> 200	70.5 ± 10.0	2.8
Doxorubicin	< 1.5	20.2 ± 2.5	14.0 ± 1.1	0.14 ± 0.0	0.4 ± 0.1	NA	NA
Amphotericin B	53.8 ± 7.0	10.0 ± 1.2	NA	NA	32.2 ± 8.8	0.4 ± 0.1	134.5

Data represent the mean value ± SD (N = 3) (in μg/mL) of the median lethal concentration (LC$_{50}$) and the median effective conentration (EC$_{50}$). MDMhu: Human monocyte-derived macrophages; MPha: Hamster´s peritoneal macrophages; Caco-2 human colon adenocarcinoma cell line; Detroit 551: Human skin fibroblast cell line; NA: No apply; IS: Index of Selectivity calculated in huMDM cells by LC$_{50}$/EC$_{50}$; C$_6$I: Quaternary halomethylated ammonium iodide; PC$_6$I: Quaternary halomethylated ammonium iodide incorporated in Precirol® nanoparticles.
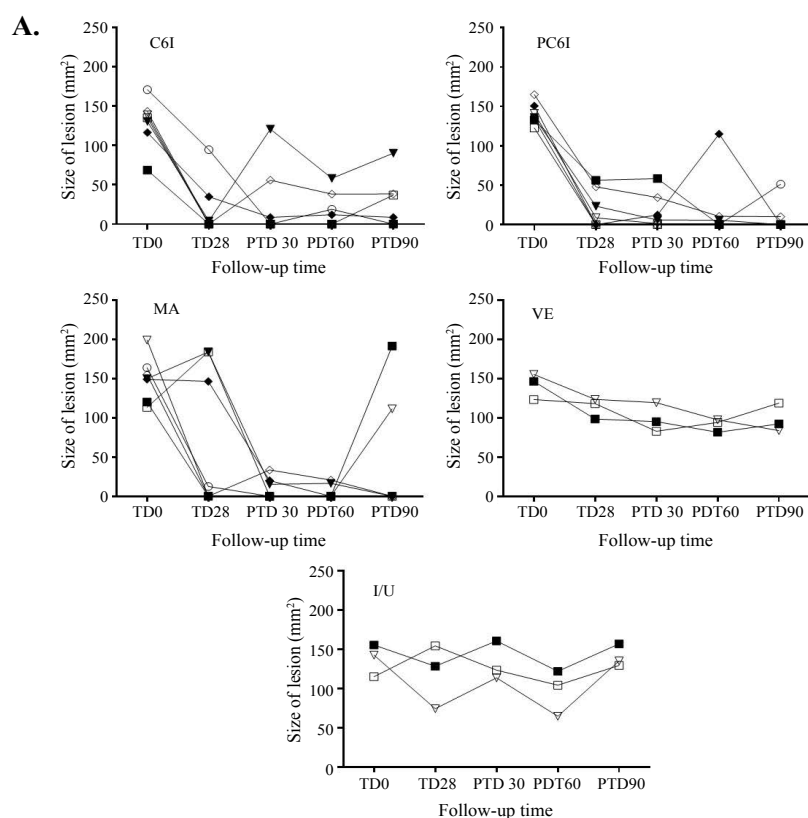

Figure 5: Response of hamsters after treatment with free quaternary halomethylated ammonium iodide and incorporated in Precirol® nanoparticules vs. meglumine antimoniate. (A) The graphs show the outcomes of hamsters after treatment with oral free C$_6$I, Precirol® NP with C$_6$I (PC$_6$I), intramuscular meglumine antimoniate (MA) or vehicle (VE) in comparison with infected and untreated hamsters. Evaluations were done at the end of treatment and post-treatment days 30 (PTD30), 60 (PTD60) and 90 (PTD90). Data represent the size of lesions at each time of follow-up. (B) Treatment progress of cutaneous leishmaniasis caused by *L. (V) braziliensis* in one hamster treated with C$_6$I and one treated with PC$_6$I (a) Before treatment (TD0); (b) On day 28 at the end of treatment (TD28) and (c) on day 90 post treatment (PTD90).
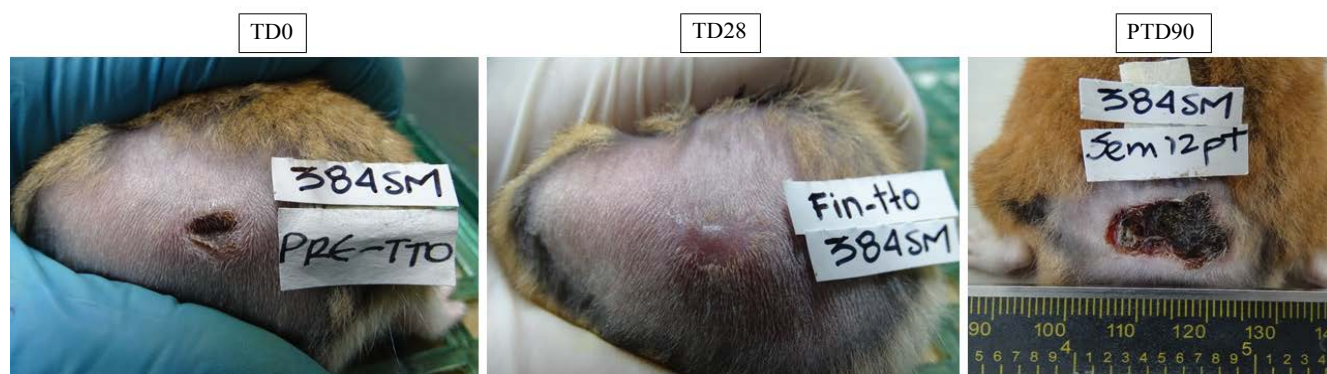
Figure 6: *In vivo* effect of free quaternary halomethylated ammonium iodide and incorporated in Precirol® nanoparticules. The figure shows representative images of a skin injury caused after injection of 5×10^7 by *Leishmania (V) braziliensis* in one hamsters and their evolution after treatment with PC_6I at 30 mg/kg/day during 28 days. (a) appearance of lesion before treatment (TD0); (b) appearance of lesion at the end of treatment (TD28) and (c) appearance of skin 90 days after treatment ended (PTD90). Notice the decrease in size after treatment and the development of scar tissue after cure.
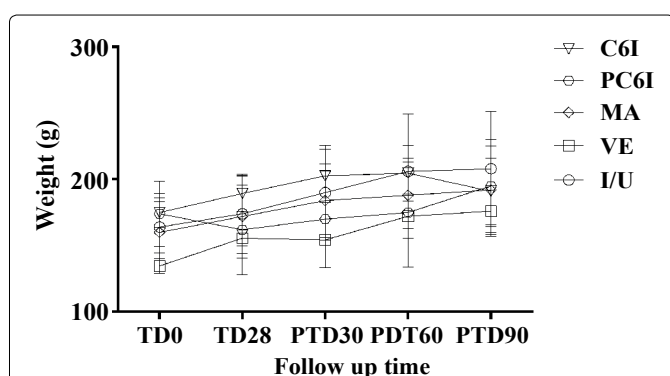

Figure 7: Effect of treatment in the weight of hamsters. The figure shows the evolution of the weight of hamsters in each group of treatment. Data represents the mean value ± SD of the weight in grams of hamsters in each experimental group: oral free C_6I; Oral Precirol® NP with C_6I (PC_6I); Intramuscular meglumine antimoniate (MA), Vehicle (VE) or Untreated (I/U).

an EC_{50} of 0.4 ± 0.2. The ratio of cytotoxicity and activity (LC_{50}/EC_{50}) showed an IS of 0.53 and higher than 500 µg/mL for C_6I and PC_6I, respectively. These results suggest that the selectivity of C_6I for the parasite increased significantly when was incorporated into the Precirol® NPs (Table 3).

Evaluation of *in vivo* effectiveness: After experimental infection, hamsters developed a single lesion ranged from 113.5 to 199.3 mm². The treatment of hamsters with free C_6I, administered orally at a dose of 30 mg/kg/day for 28 days, resulted in complete healing of ulcers in 3 animals (42.9%) at the end of the study (Figure 5). The remained hamsters that did not cure showed improvement with a reduction in the size of their lesions in 90.4, 38.4, 37.05 and 8.6%. On the other hand, the treatment of hamsters with PC_6I, administered orally at the same dose during 28 days increased the cure rate to 85.7% corresponding to 6 of 7 hamsters with complete healing of ulcers. The remained hamster of this group showed a decrease in the lesion of 95.9% (hamster PC_6I-5, Figure 5). One of cured hamster had relapse at the end of the study (hamster PC_6I-7, Figure 5) for a definitive cure

rate of 71.4% for PC_6I treatment. Although all hamsters treated with intramuscular injections of MA showed cure during the study, only 5/7 (71.4%) hamsters remained cured at the end of the study while the last two hamsters had relapses of their ulcers. As expected, any hamster from the vehicle treated or untreated groups resolved their lesions during the study (Figure 5A). The appearance of lesion in hamsters prior and after treatment with C_6I and PC_6I and at the end of the study are shown in Figure 5B, Figure 6.

The parasite load expressed as at the end of the study in the ulcers by group of treatment was 644.4 ± 953.8 parasites/mg of tissue (mean ± SD, n = 7) and 303.2 ± 288.6 parasites/mg of tissue in hamsters treated with C_6I and PC_6I, respectively. These difference was statistically significant (p < 0.01).

Toxicity in hamsters after treatment: The hamsters gained weight during the study and no statistically significant differences were observed among groups (Figure 7). Serum levels for all animals of ALT, BUN, and CRT were within the range of normal values for all animals both before (TD0) and after (PTD8) the all treatments (Figure 8).

Oral toxicity at repeated doses (28 days): No deaths or disabling events were neither registered nor clinical signs associated with toxicity of the compounds. The behavior of the mice and their physical appearance were normal even after the administration of the substances. Mice were attentive to the medium, exploring in the cages, grooming each other or adopting typical positions to rest or sleep. Mice treated with free C_6I at 30 mg/kg/day showed alterations at the gastrointestinal level with soft stools from the middle of the study to the end without affect the body weight. At contrary, at the end of the study all treated with free C_6I or PC_6I presented weight gain. At necropsy, only hepatic liver-type changes were reported in two animals of the PC_6I group. At the histological level, slight vacuolar degeneration was observed in the kidney, liver and small
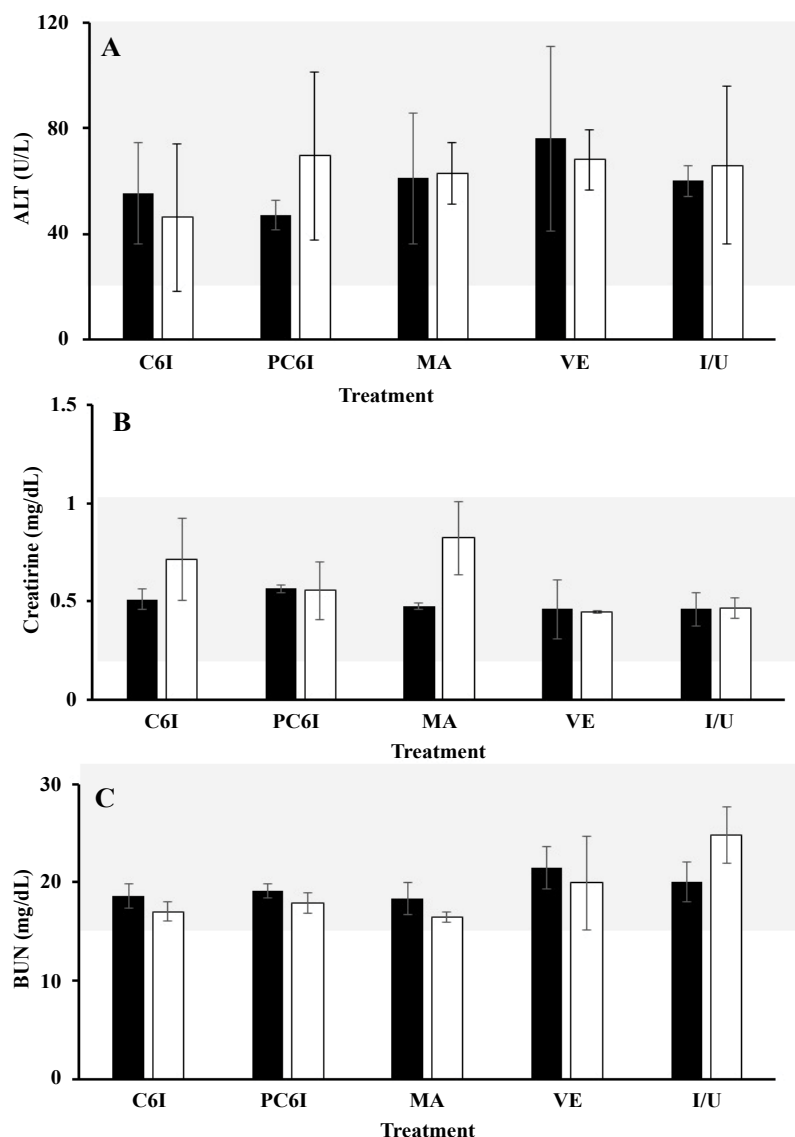
Figure 8: Comparison of BUN, creatinine and ALT Level in serum of hamsters treated with free quaternary halomethylated ammonium iodide and incorporated in Precirol® nanoparticules *vs.* meglumine antimoniate. (a) Comparison of ALT BUN (b) and creatinine (c) in serum of treatment groups before (TD0) and 8 days after treatment ended (PTD8) in hamsters with cutaneous leishmaniasis. Data are shown as median ± SD. No significant differences were seen between groups ($p > 0.05$). Precirol® nanoparticles incorporating C_6I (PC_6I); meglumine antimoniate (MA); Empty Precirol® nanoparticles (VE); Infected and untreated hamsters (I/U). No differences were observed neither among individuals in each group nor between groups. Dotted lines in red delimit the reference values.

intestine while slight hyperplasia was observed in liver and spleen of some hamsters treated with both C_6I and PC_6I. The hematological parameters and serum levels of ALT, AST, CRT and BUN were within the reference values indicating no alterations in the kidney and liver function for both treatments.

Discussion

One of the objectives pursued for the treatment of leishmaniasis is the development of more effective and safer active pharmaceutical ingredients that can be administered topical or orally to ensure greater acceptance by patients. Previously studies of the quaternary halomethylated ammonium iodide C_6I meets the requirements mentioned previously. Our study continued with the pharmacological characterization; the C_6I exhibited low dissolution profile with a IDR value similar

in the three different pH, additionally the DSC and DRX analysis confirmed that C_6I presented a crystalline structure, as described by others authors [7,8]. This crystalline lattice is mainly due to the presence of aromatic rings, which tend to form strong and organize crystalline structure, compounds with this type of structure as usual they present low solubility and dissolution [8,9].

The Doluisio method showed good intestinal permeability of C_6I, with *Papp* one order of magnitude greater than that showed by metoprolol (5.6×10^{-6} cm/s) and in the same range of ibuprofen, which are drugs with good intestinal permeability [10]. On the other hand, rate constants (k_a) were the first order, which showed the intestinal absorption of C_6I was a passive diffusion process, since there were no statistically significant differences between the constants of the two concentra-

tions tested [23]. The passive diffusion of C_6I is favored by its small molecular weight, positive charge and moderate polarity. Some authors report that compounds with positive charge and molecular weight below 400 Da could access at intestinal epithelium through paracellular pathway [24,25]. Together these results and those reported previously [5] allowed to classify the C_6I as type 2 compound according to the biopharmaceutical classification system (BCS), with low solubility and good intestinal bioavailability. In turn, the bioavailability of type 2 compounds can affect the amount of drug in solution as well as the amount of C_6I that can be absorbed at gastrointestinal level; therefore, type 2 compounds should adapt new strategies to improve their gastrointestinal biopharmaceutical profile, with the purpose to increase the amount of compound bioavailable at systemic level [26].

In acute and repeated doses were evidenced slight edema, vascular congestion and vacuolar degeneration. Despite these signs, organ size and serum metabolites related to hepatic function were normal. On the other hand, C_6I did not show mutagenic activity in the *S. typhimurium* model (TA98 and TA100 strains) and nor chromosomal alterations in human lymphocytes. These results are similar to those showed by other quaternary ammonium compounds [27].

In this work, we use Precirol® not only because it allows the manufacture of NPs easily and economically and by storage conditions, but mainly because it allows the controlled release of drugs [8,28]. The Precirol® NPs improved the pharmaceutical profile (higher effectiveness and lower toxicity) and the biopharmaceutical profile (bioavailability) for C_6I as demonstrated by others [29,30].

The C_6I was solubilized in a small amount of dichloromethane before the incorporation in the lipid phase. Using 3 mg of C_6I, the percentage of encapsulation was higher than 60%. Although the zeta potential was outside the desired range (+30 to -30) [31], the obtained values still indicate good colloidal stability, considering the steric stabilization given by the Tween 20 used as surfactant [32].

The stability tested showed, the storage condition, autoclave conditions and DLS test did not change significantly the mainly characteristics of formulation as size and encapsulation capacity. Authors reported the SLNs as stable systems in different conditions [33]. In contrast, the zeta potential was significantly lower which may be due to a reorganization of the polymorphic transitions of the lipid matrices with subsequent rearrangement of the compound within the formulation [8,28,29].

The DSC analyses showed a rearrangement of the particles compared with the bulk product. The change in the DSC profile could be due to possible defects in the lipid network, leading to a decrease in their crystallinity compared with their bulk counterparts [34]. Thus,

for less ordered or amorphous crystals, the fusion of the substance requires much less energy than that for crystalline substances. Additionally, the crystallization processes during the production are complex and strongly dependent on the lipid composition and production conditions as they directly affect the location of the active compound within the particle and its release profile [35]. After 24 hours the 96% of C_6I was released, being exponential and faster during the first hour possibly due to the presence of molecules of the compound on the surfaces of the particle. After 2 hours the released was delayed possibly due to the diffusion of C_6I dissolved in the nucleus of the nanoparticles in the dissolution medium.

In this work, the release profile showed that C_6I improved its solubility in solution when it was incorporated into Precirol® NPs compared to the results of the intrinsic dissolution of pure free C_6I. According with the IDR value, 0.24 mg of compounds per centimeter was dissolved each minute, while the release and dissolution of C_6I in the nanoparticles occurred rapidly in the first hours and more than half of the compound was in solution. According to Noyes-Whitney and Ostwald-Freundlich principles, the particle size in the nanometer range can lead to an increased dissolution velocity and saturation solubility for a nanoformulation. Previous studies with a number of poorly soluble drugs have demonstrated that particle size reduction can lead to an increased rate of dissolution and higher oral bioavailability [8,29,36].

On the side of toxicity and effectiveness, our results showed a significant decrease in the toxicity but an increase of antileishmanial activity for intracellular amastigotes of *L. (V) braziliensis* of C_6I when incorporated in Precirol® NPs. In this case, the EC_{50} of PC_6I was 40-fold lower than free C_6I. Additionally, previous studies *in vivo* demonstrated that C_6I was able to cure hamsters with CL by *L. (V) panamensis* when administered topically at a dose of 2 mg/kg/day for 15 days [5]. Here we show that free C_6I, administered orally at a dose of 15 mg/kg/day for 28 days, showed an effectiveness close to 30%. Nevertheless, its effectiveness increased to 71% when the C_6I was incorporated in Precirol® NPs and administered at a higher dose of 30 mg/kg/day. The results were consistent in the *in vivo* model, with 71% cure in the group of animals treated with PC_6I upon oral administration of a dose of 30 mg/kg/day for 28 days. Differences in the effectivity and toxicity between free C_6I or encapsulated PC_6I was evident not only because the LC_{50} increased two-fold but also because the EC_{50} was lowered 40-fold. Several hypotheses may explain how the SLN improve de effectivity of compound. We hypothesize that the solubility and dissolution of pure compound was low so that the concentration available in polar and physiological solutions is few. Possibly, nanoparticles loaded with C_6I increased the dissolution of compound and improved the solubility in polar solutions, for example, culture medium, and thus, more compound was avail-

able to enter in the infected cell. In the case *in vivo* test it is possible that compound was soluble in GI solutions and thus, the dissolved C_6I is able to cross the intestinal wall and to reach the systemic circulation and its target [8,14,29,37]. Furthermore, SLNs used for oral administration offer several benefits over conventional formulations including increased solubility, enhanced stability, improved epithelium permeability and bioavailability, prolonged half-life, tissue targeting, and minimal side effects as well as the potentiating effect of the antileishmanial activity [8,28].

The *in vivo* activity of free C_6I or incorporated in the Precirol® NPs (PC_6I) was tested in the hamster because this is the most adequate animal model for CL by *Leishmania* species of *Viannia* subgenus. The effectiveness was compared with the intramuscular MA instead miltefosine because MA is able to resolve CL in the hamster model infected with *L. (V) braziliensis* at the dose used in this study [20] while miltefosine has not shown any cure [38]. Despite the use of different administration routes, both treatment with the salts and the MA are systemic and this validates the use of MA as a control. On the other hand, although the days of treatment were different (28 *vs.* 10 for the salts *vs.* MA), the efficacy of the treatments was evaluated based on the outcome of the cure observed after the treatment was finished. In this way, day 0 of follow-up began one day after the end of the treatment, regardless of the duration of the treatment. Moreover, the treatment for all groups was safe during 28 days of administration and during 90 days of follow-up; the hamsters gained weight and levels of ALT, BUN, and CRT were within the range of normal values for all animals both before (TD0) and after (PTD8) treatment.

Additionally, in all assays where the safety profile was tested, the compound was safe. This profile was studied in rats and mice as recommended in the international guides; in this way it is also guaranteed that the non-toxicity of the substance does not depend on the species tested. We also showed that this activity is selective, *in vitro* being potentially non-toxic for colon Caco-2 cells and for primary cultures of human macrophages huMDM, which suggest that C_6I does not affect the colon cells during the process of intestinal absorption nor the host cells for *Leishmania* parasites during treatment. Moreover, the NPs improved the cytotoxicity of the free C_6I increasing the LC_{50} in 21 times for the U937 and MPha. The LC_{50} for Caco-2 and huMDM were similar. The *in vivo* oral acute toxicity results defined the maximum concentration to evaluate the effect after oral administration at repeated doses (28 days). There were no deaths or changes in body weight, as well as anatomical changes at necropsy that could be associated with a possible toxicity for C_6I. The PC_6I formulation presented a pattern of safety as shown by results obtained in organs such as heart, spleen, intestine, brain and reproductive organs, as well as the blood chemistry profile without evident toxic manifestations. Although, two animals had fatty liver and at the histological level, events such as congestion and mild to moderate vacuolar degeneration were observed, it is known that NP systems induce oxidative stress in the liver [39]. Additionally, the presence of a cationic surfactant may generate some cytotoxicity [40].

In conclusion, despite the low solubility and the dissolution profile shown by C_6I, the compound possesses other physicochemical, pharmacokinetic and pharmaceutical properties that make it suitable for the oral formulation. The C_6I showed good intestinal permeability and potential no toxicity after oral administration in the murine model. The genotoxicity or mutagenicity of C_6I were absent. The Precirol® NPs was a suitable strategy that improved not only the bioavailability and toxicity but also the effectiveness of the C_6I both *in vitro* and *in vivo*. Indeed, the cure rate of hamsters with experimental CL increased from 30% to 71% after daily administration for up to 28 days. Results showed here confirm that the PC_6I formulation has high potential to become a new drug for the treatment of CL.

Authors´ Contribution

MF, TG, AA, SMR carried out the experiments. The manuscript was prepared by MF, SMR. All authors analyzed the data, discussed the results and revised the manuscript.

Conflict of Interest

The authors declare that there is no conflict of interest in this work.

Funding

Acknowledgements

References

1. Alvar J, Velez ID, Bern C, Herrero M, Desjeux P, et al. (2012) Leishmaniasis worldwide and global estimates of its incidence. PLoS one 7: e35671.

2. Yamey G (2002) The world's most neglected diseases: Ignored by the pharmaceutical industry and by public-private partnerships. BMJ 325: 176.

3. Duque-Benitez SM, Rios-Vasquez LA, Ocampo-Cardona R, Cedeno DL, Jones MA, et al. (2016) Synthesis of novel quaternary ammonium salts and their in vitro antileishmanial activity and U-937 cell cytotoxicity. Molecules 21: 381.

4. Rios LA, R Ocampo, SM Duque, SM Robledo, ID Velez DL, et al. (2015) Quaternary N-(halomethyl) ammonium salts as therapeutic agents. Patent.

5. Fernandez M, Murillo J, Rios-Vasquez LA, Ocampo-Cardona R, Cedeno DL, et al. (2018) In vivo studies of the effectiveness of novel N-halomethylated and non-halomethylated quaternary ammonium salts in the topical treatment of cutaneous leishmaniasis. Parasitol Res 117: 273-286.

6. Pulido SA, Nguyen VH, Alzate JF, Cedeno DL, Makurath MA, et al. (2017) Insights into the phosphatidylcholine and phosphatidylethanolamine biosynthetic pathways in Leishmania parasites and characterization of a choline kinase from Leishmania infantum. Comparative Biochemistry and Physiology Part B: Biochemistry and Molecular Biology 213: 45-54.

7. Zakeri-Milani P, Barzegar-Jalali M, Azimi M, Valizadeh H (2009) Biopharmaceutical classification of drugs using intrinsic dissolution rate (IDR) and rat intestinal permeability. Eur J Pharm Biopharm 73: 102-106.

8. Lin CH, Chen CH, Lin ZC, Fang JY (2017) Recent advances in oral delivery of drugs and bioactive natural products using solid lipid nanoparticles as the carriers. Journal of food and drug analysis 25: 219-234.

9. Wood JH, Syarto JE, Letterman H (1965) Improved holder for intrinsic dissolution rate studies. Journal of pharmaceutical sciences 54: 1068-1068.

10. Doluisio JT, Billups NF, Dittert LW, Sugita ET, Swintosky JV (1969) Drug absorption I: An in situ rat gut technique yielding realistic absorption rates. Journal of pharmaceutical sciences 58: 1196-1200.

11. https://www.oecd-ilibrary.org/environment/test-no-471-bacterial-reverse-mutation-test_9789264071247-en

12. https://www.oecd-ilibrary.org/environment/test-no-473-in-vitro-mammalian-chromosomal-aberration-test_9789264264649-en

13. https://www.oecd-ilibrary.org/environment/test-no-407-repeated-dose-28-day-oral-toxicity-study-in-rodents_9789264070684-en

14. Vitorino C, Carvalho FA, Almeida AJ, Sousa JJ, Pais AA (2011) The size of solid lipid nanoparticles: An interpretation from experimental design. Colloids and Surfaces B: Biointerfaces 84: 117-130.

15. Lopes R, Eleuterio CV, Goncalves LMD, Cruz MEM, Almeida AJ (2012) Lipid nanoparticles containing oryzalin for the treatment of leishmaniasis. European Journal of Pharmaceutical Sciences 45: 442-450.

16. International Conference on Harmonization of Technical Requirements for Registration of Pharmaceuticals for Human (ICH) (2005) Harmonised tripartite cuideline: Validation of analytical procedures: Text and methodology, Q2(R1). In: International Conference on Harmonization of Technical Requirements for Registration of Pharmaceuticals for Human Use.

17. Mesa CV, Blandon GA, Munoz DL, Muskus CE, Florez AF, et al. (2015) In silico screening of potential drug with antileishmanial activity and validation of their activity by in vitro and in vivo studies. J Chem Chem Eng 9: 375-402.

18. Finney DJ (1964) Statistical Method in Biological Assay. In: Charles Griffin Co. (2nd edn), London.

19. Pulido SA, Munoz DL, Restrepo AM, Mesa CV, Alzate JF, et al. (2012) Improvement of the green fluorescent protein reporter system in Leishmania spp. for the in vitro and in vivo screening of antileishmanial drugs. Acta tropica 122: 36-45.

20. Robledo SM, Carrillo LM, Daza A, Restrepo AM, Munoz DL, et al. (2012) Cutaneous leishmaniasis in the dorsal skin of hamsters: A useful model for the screening of antileishmanial drugs. J Vis Exp.

21. Ribeiro-Romao RP, Saavedra AF, Da-Cruz AM, Pinto EF, Moreira OC (2016) Development of real-time PCR assays for evaluation of immune response and parasite load in golden hamster (Mesocricetus auratus) infected by Leishmania (Viannia) braziliensis. Parasit Vectors 9: 361.

22. https://www.oecd-ilibrary.org/environment/test-no-421-reproduction-developmental-toxicity-screening-test_9789264264380-en

23. Lennernas H (2007) Animal data: The contributions of the Ussing Chamber and perfusion systems to predicting human oral drug delivery in vivo. Adv Drug Deliv Rev 59: 1103-1120.

24. Adson A, Raub TJ, Burton PS, Barsuhn CL, Hilgers AR, et al. (1994) Quantitative approaches to delineate paracellular diffusion in cultured epithelial cell monolayers. J Pharm Sci 83: 1529-1536.

25. Palm K, Luthman K, Ros J, Grasjo J, Artursson P (1999) Effect of molecular charge on intestinal epithelial drug transport: PH-dependent transport of cationic drugs. J Pharmacol Exp Ther 291: 435-443.

26. https://www.fda.gov/downloads/Drugs/GuidanceComplianceRegulatoryInformation/Guidances/UCM070246.pdf.

27. Xue Y, Hieda Y, Kimura K, Takayama K, Fujihara J, et al. (2004) Kinetic characteristics and toxic effects of benzalkonium chloride following intravascular and oral administration in rats. J Chromatogr B Analyt Technol Biomed Life Sci 811: 53-58.

28. Pham TTH, Loiseau PM, Barratt G (2013) Strategies for the design of orally bioavailable antileishmanial treatments. International journal of pharmaceutics 454: 539-552.

29. Hoshyar N, Gray S, Han H, Bao G (2016) The effect of nanoparticle size on in vivo pharmacokinetics and cellular interaction. Nanomedicine 11: 673-692.

30. Almeida AJ, Souto E (2007) Solid lipid nanoparticles as a drug delivery system for peptides and proteins. Adv Drug Deliv Rev 59: 478-490.

31. Iqbal MA, Md S, Sahni JK, Baboota S, Dang S, et al. (2012) Nanostructured lipid carriers system: recent advances in drug delivery. J Drug Target 20: 813-830.

32. Freitas C, Muller RH (1999) Correlation between long-term stability of solid lipid nanoparticles (SLN™) and crystallinity of the lipid phase. Eur J Pharm Biopharm 47: 125-132.

33. Muller RH, MaEder K, Gohla S (2000) Solid lipid nanoparticles (SLN) for controlled drug delivery–a review of the state of the art. European journal of pharmaceutics and biopharmaceutics 50: 161-177.

34. Gaspar DP, Faria V, Goncalves LM, Taboada P, Remunan-Lopez, et al. (2016) Rifabutin-loaded solid lipid nanoparticles for inhaled antitubercular therapy: Physicochemical and in vitro studies. Int J Pharm 497: 199-209.

35. Lopes RM, Gaspar MM, Pereira J, Eleuterio CV, Carvalheiro M, et al. (2014) Liposomes versus lipid nanoparticles: Comparative study of lipid-based systems as oryzalin carriers for the treatment of leishmaniasis. Journal of biomedical nanotechnology 10: 3647-3657.

36. Hintz RJ, Johnson KC (1989) The effect of particle size distribution on dissolution rate and oral absorption. International Journal of Pharmaceutics 51: 9-17.

37. Horter D, Dressman JB (2001) Influence of physicochemical properties on dissolution of drugs in the gastrointestinal tract1. Adv Drug Deliv Rev 46: 75-87.

38. de Morais-Teixeira E, Aguiar MG, Soares de Souza Lima B, Ferreira LAM, Rabello A (2015) Combined suboptimal schedules of topical paromomycin, meglumine antimoniate and miltefosine to treat experimental infection caused by Leishmania (Viannia) braziliensis. J Antimicrob Chemother 70: 3283-3290.

39. Lawrence XY, Carlin AS, Amidon GL, Hussain AS (2004) Feasibility studies of utilizing disk intrinsic dissolution rate to classify drugs. Int J Pharm 270: 221-227.

40. Lewinski N, Colvin V, Drezek R (2008) Cytotoxicity of nanoparticles. Small 4: 26-49.

Fernández et al. Int Arch Med Microbiol 2018, 1:007

• Page 14 of 14 •